Numerical study of the influence of the Reynolds-number on the lift created by a leading edge vortex

Xiaoqin Zhang and Jörg U. Schlüter

Citation: Physics of Fluids (1994-present) **24**, 065102 (2012); doi: 10.1063/1.4718322
View online: http://dx.doi.org/10.1063/1.4718322
View Table of Contents: http://scitation.aip.org/content/aip/journal/pof2/24/6?ver=pdfcov
Published by the AIP Publishing

Numerical study of the influence of the Reynolds-number on the lift created by a leading edge vortex

Xiaoqin Zhang[a] and Jörg U. Schlüter
Nanyang Technological University, School of Mechanical and Aerospace Engineering, Singapore

(Received 8 December 2011; accepted 30 April 2012; published online 13 June 2012)

We present a numerical study on the influence of the Reynolds-number on the lift enhancing effect of a leading edge vortex. Our approach is based on a combination of large-eddy simulations and the immersed boundary technique. We determine the influence of the leading edge vortex on the unsteady lift by simulating a fast pitch-up motion of the plate and studying the lift evolution after holding the flat plate fixed at an angle of attack. Our results suggest that an optimal Reynolds-number exists that maximizes the lift of the leading edge vortex, but that the lift-to-drag ratio is largely independent of the Reynolds-number above a Reynolds-number of $Re_c > 2000$. © *2012 American Institute of Physics*. [http://dx.doi.org/10.1063/1.4718322]

I. INTRODUCTION

The flight of birds and insects has been inspiration for flight for centuries. Yet, it is difficult to match the grace and efficiency of these natural flyers and to imitate the flapping wing flight for mechanical devices, such as micro air vehicles (MAV). While conventional fixed-wing aerodynamics is well understood, the aerodynamic efficiency of airfoils and wings designed for fixed wing flight is surprisingly low at small scales and low-Reynolds-numbers.[1] Many experiments have shown that the lift produced at low Reynolds-number is relatively low.[2,3] Yet, since obviously insects demonstrate that at low Reynolds-numbers efficient flight is possible, less explored effects need to be in play to provide additional lift.

Flapping wing flight has received more interest within the last decades.[4,5] Several factors lead to the improved performance of flapping wing flyers compared to fixed-wing aircraft such as the wing-wake capture,[6] the clap-and-fling mechanism,[7] and the leading edge vortex (LEV).[8]

The main working principle of the LEV is that the low pressure in the vortex generated at the leading edge due to flapping and pitching provides an additional lift component. The LEV has been identified as a major contributor in many biological examples, such as butterflies,[9] hummingbirds,[10] bats,[11] and samara seeds.[12] The LEV has since been the subject of many studies. Amongst the most notable ones is the study of Ellington,[13] who studied the lift created on a hovering hawkmoth using a robotic model and the numerical study of Sun and Tang[14] of that same experiment. Both studies showed two distinct peaks in the lift generation. The first peak occurs during the pitching motion of the wing and can be associated to the Kramer effect,[15] which links the sudden increase in lift with the creation of circulation due to the rotational pitching motion of the wing. The second peak occurs with a time-lag as a result of the complex vortex motion due to the pitching of the wing, i.e. the LEV. Shyy and Liu[5] performed further simulations on the hawkmoth wing and identified the LEV as a dominant part in the lift generation.

A dynamic LEV can be created in the flapping cycle either by the translational or the rotational (pitching) movement. The pure pitching motion of wings has been the subject of research unrelated to the biological application. The aerodynamic characteristics of the flat plates in pitching oscillation are investigated by Han *et al.*[16] The lift coefficient on a flat plate undergoing pitching and plunging

[a]Present address: Temasek Laboratories, NUS, Singapore.

motion is presented in comparison with the one on airfoil SD7003 by Kang *et al.*,[17] which is also investigated in experiments by Baik *et al.*[18]

Eldredge and Wang[19] have studied a thin flat plate undergoing a rapid pitch-up at Reynolds-number 1000 with numerical simulations. The effect of pitching rate and axis position of pitching is inspected. They concluded that both maximum drag and lift increase as pitch rate increases, but this increase diminishes as the pitch axis is moved aft. A review of recent work on "canonical" pitch motions using both experimental and numerical techniques has been given by Ol *et al.*[20] Some earlier investigations on rapidly pitching airfoils have been reported (e.g., in Refs. 21 and 22). Lentik and Dickinson have performed measurements on the LEV at different Reynolds-numbers and stated that the lift due to the LEV is independent at $\mathrm{Re}_c > 1400$, but determined an aerodynamic performance loss at very low Reynolds-numbers.[23]

In the present work, we would like to study the influence of the Reynolds-number on the transient LEV. We rapidly pitch the flat plate up and keep it fixed at an angle of attack. We then study the temporal evolution of the LEV and the lift force due to the LEV focusing here especially on the initial generation of the LEV. To investigate the dependency of Reynolds-number, four chord-based Reynolds-numbers $\mathrm{Re}_c = 440$, $\mathrm{Re}_c = 2000$, $\mathrm{Re}_c = 6000$ and $\mathrm{Re}_c = 21\,000$ are considered. They are comparable with those of fruit flies, bees, dragonflies, and small birds (or bats), respectively. For each Reynolds-number, six terminal angles of attack are studied.

II. NUMERICAL APPROACH

Our approach to simulate the pitching plate is to use large-Eddy simulations (LES) combined with the immersed boundary (IB) technique. In the LES approach, the large energy containing vortices, such as the LEV, are resolved directly in time and space without modeling. Other than unsteady Reynolds-averaged Navier-Stokes turbulence models, which tend to introduce too much dissipation at the large eddies, in LES only the smallest, energy dissipating eddies need to be modeled and hence, the creation, evolution and destruction of the LEV is resolved in its entirety. Yet, due to the dissipation of the smallest eddies with an appropriate LES model, higher Reynolds-numbers can be simulated without the prohibitively high cost of direct numerical simulations. This allows to study not only the Reynolds-number range of insects as in previous studies (e.g., Ref. 24), but also the Reynolds-number range of birds and bats, which is especially interesting for the application to MAV.

Furthermore, the effects we study are in a transitional range, which means that we need to simulate the time-evolving flow in the laminar regime equally as in the turbulent regime. This also requires an LES subgrid scale model that reduces to zero in laminar flows. We use the dynamic sub-grid scale model of Germano *et al.*[25] and Lilly,[26] which does not require external constants. As the model constants are determined from the solution, the influence of the subgrid scale model is reduced to zero in laminar flows.

To solve the Navier-Stokes equation for the unsteady incompressible flows, the IB method[27] is used instead of a conventional body-conformal method. In the IB method, the governing equations are discretized on a simple Cartesian grid with no regard to the object immersed in the fluid domain. The no-slip boundary condition at the immersed boundary is enforced by modification of the governing equation. The use of a Cartesian grid greatly simplifies grid generation and saves effort in coordinate transformation. All the advantages of a structured mesh are retained without issues related to skewness and distortion of an unstructured mesh. When the object immersed in the fluid moves, it is sufficient to use only one mesh during the entire simulation. In contrast, methods using the body-conformal grids require a new mesh to be generated at each time step and the solution has to be interpolated from the old mesh onto the new mesh. Thus, the computational cost of IB method is reduced significantly. The method was originally developed by Peskin[27] to simulate blood flow and has since been used for many other problems in biophysics, and lately turbulent flows around rigid bodies. Flows with complex moving boundaries, such as a diaphragm-driven micropump with moving valves, have been studied by Udaykumar.[28] Fadlun *et al.*[29] applied this approach in the framework of a finite-difference LES code to vortex ring formation, to the flow around a sphere and to a more complex piston/cylinder assembly. Thereafter, Verzicco *et al.* used the same code to simulate the three-dimensional flow around a road vehicle[30] and the flow in an impeller-stirred tank.[31]

Here, we adopt the forcing approach by Mohd-Yusof[32] to account for the presence of the immersed boundary. The Lagrangian method[33] has been employed as a special treatment for the freshly cleared cells, which are the cells located in the external domain at one time step and emerge to the fluid at the next time step. It is used to compute the material derivative of the velocity on the freshly cleared grid points in a Lagrangian coordinate system.

The LES solver used in the current work was originally developed by Dr. Charles Pierce[34,35] at Stanford University. The solver is based on a finite volume method using a staggered grid. The code has been validated on a wide variety of flows.[36–39] We have added the IB method to the solver and validated it on stationary and transient problems.[33,40,41]

III. COMPUTATIONAL SETUP AND PROCEDURES

A flat-plate of chord length c with 7% thickness is placed in the fluid with the plate center at the origin. The computational domain spans from $-2.5c$ to $3.0c$ in streamwise (x), $-2.5c$ to $2.5c$ in vertical (y) direction. It has a width of $2c$ in spanwise (z) direction. We have computed the cross-correlation of the spanwise velocity component at $\mathrm{Re}_c = 6000$ and found that the correlation of the signal does not extend further than $0.3c$, and as such we deem the choice of the spanwise extend justified as the size of turbulent structures are much smaller than the crosswise domain size. The upper and lower boundaries are set to free-slip walls. In spanwise direction, periodic boundary conditions are applied. A laminar plug flow profile with additional 10% turbulent perturbation of the bulk velocity is generated as inflow condition, with the turbulent fluctuations generated by a precursor simulation of a turbulent channel flow at $\mathrm{Re}_H = 10\,000$.[38] The main goal of the additional turbulent fluctuations is to allow the development of three-dimensional structures that would otherwise not be observed. The Cartesian grid is clustered around the flat plate in order to resolve the boundary layer. 15 grid points are placed across the plate thickness. Equidistant mesh of 32 points is used in spanwise direction. The mesh has around 3.5×10^6 cells in total. First, simulations are performed with the flat plate in horizontal position for $\Delta t^* = 5.0$ to create an initial condition, where a $\Delta t^* = 1.0$ denotes the time required for the flow at freestream velocity U_∞ to travel across the length of the flat plate c (i.e. $t^* = U_\infty t/c$). Then, we rotate the flat plate from zero degree to a determined angle α with a rotational speed $2/3\pi$ ($=120^\circ$) per non-dimensional unit time and keep the plate frozen at the terminal angle of attack α. The center of rotation is the center of the flat-plate. To study the influence of angle of attack, simulations are performed for terminal angles of attack from $\alpha = 5^\circ$ up to $\alpha = 30^\circ$ with $\Delta\alpha = 5^\circ$.

In order to determine the contribution of the LEV on the lift, we determine the temporal evolution of the lift coefficient. During the motion phase of the flat plate the lift coefficients increase significantly, since the motion of the flat plate introduces circulation into the flow due to the Kramer effect (Figure 1). While this motion can create much of the lift that is being produced in flapping wing flight, it requires work to be done onto the flow. Additional peaks at the beginning and end of the motion phase can be seen as well and are due to the acceleration of the flat plat from rest (Wagner effect).[42] In the current study, we would like to focus on the peak after the motion has stopped, which, as our flow visualizations reveal, coincides with the creation and passing of the LEV. It is advantageous to make use of the LEV, as no additional work is required to obtain the lift that goes along with it.

The simulations are run for a non-dimensional time span of $\Delta t^* = 35.0$ and averaged over the last $\Delta t^* = 25.0$ to determine the mean value (Figure 2). As a test to ascertain that the averaging time span is sufficient, we have determined the mean value over the last $\Delta t^* = 10.0$ and observe that the mean value varies less than 4% for all simulations from the mean value using the longer averaging time-span. The lift contribution of the LEV is determined as the maximum value obtained after the pitch-up motion is completed. The additional lift due to the LEV can then be determined with the dynamic component of the lift.

IV. RESULTS

Figure 3 shows the evolution of the spanwise vorticity for four Reynolds-numbers, while Figure 4 shows the corresponding development of the dynamic lift component $C_{l,dyn}$. The

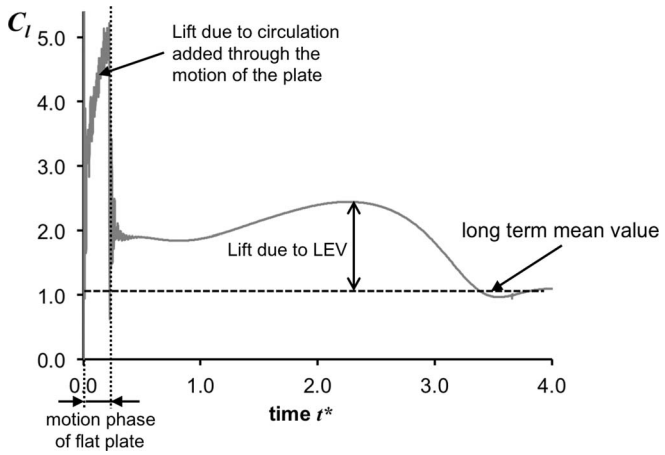

FIG. 1. Temporal evolution of the lift coefficient in the initial phase at the example of $\mathrm{Re}_c = 440$ and $\alpha = 25^\circ$.

visualization in Figure 3 shows that the LEV at $\mathrm{Re}_c = 440$ as a coherent structure undisturbed by small-scale turbulence. At this low Reynolds-number viscosity plays a major role, and prohibits the generation of smaller vortices. However, the high viscosity also attenuates the main LEV. This leads to less lift generated, as shown in Figure 4, in comparison with higher Reynolds-numbers. The LEV at $\mathrm{Re}_c = 21\,000$ is less coherent (see Figure 3), as the higher Reynolds-number permits the generation of smaller secondary vortices. Despite the fact that the smaller vortices disturb the evolution of the larger main LEV, the lift generated from the LEV is higher than compared to very low Reynolds-numbers (see Figure 4), as the main LEV is mainly unaffected by the viscosity, albeit being disturbed by the generated small-scale turbulence. Hence, there must be an intermediate optimal case, where the viscosity is sufficiently low as to not disturb the creation of the main LEV, but sufficiently large as to inhibit the generation of small-scale turbulence. As can be seen in Figure 3, at $\mathrm{Re}_c = 6000$, the main LEV is well developed but still mildly disturbed by small-scale turbulence. At $\mathrm{Re}_c = 2000$, the creation of the LEV seems the least affected by small-scale turbulence.

Figure 5 shows the three-dimensional vortex structure of the LEV. The LEV is visualized by isosurfaces of the q-criterion as defined by Haller.[43] At $\mathrm{Re}_c = 440$, no three-dimensional structures can be identified. The flow is virtually two-dimensional and no secondary longitudinal structures develop. At $\mathrm{Re}_c = 2000$, the LEV is slightly disturbed by the presence of longitudinal streaks. These streaks hardly affect the LEV. At Reynolds numbers above $\mathrm{Re}_c = 6000$, chaotic three-dimensional

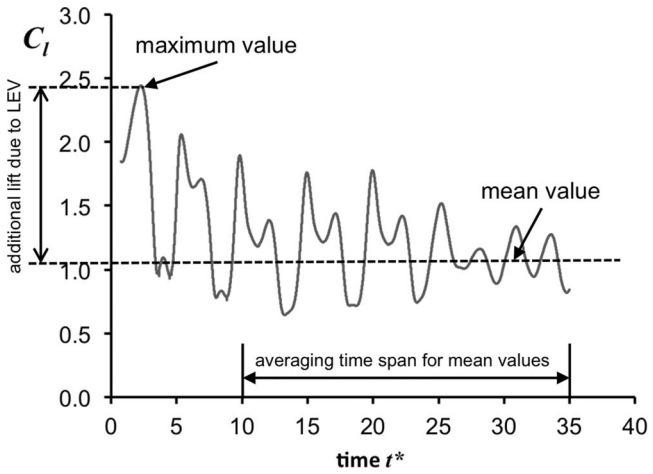

FIG. 2. Procedure to determine maximum and average lift coefficient at the example of $\mathrm{Re}_c = 440$ and $\alpha = 25^\circ$.

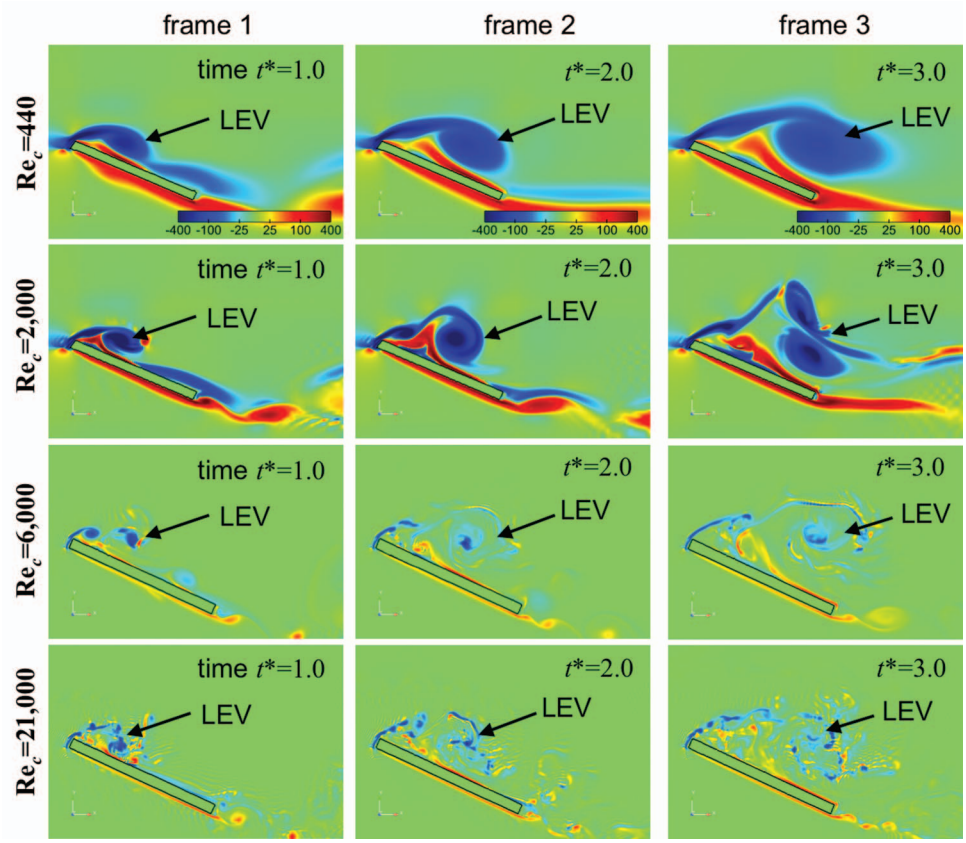

FIG. 3. Spanwise vorticity of the flow over a flat-plate pitched up to $\alpha = 25^\circ$.

turbulence is dominating the flow field around the LEV. Some longitudinal streaks can be identified, however, the streaks disintegrate soon after their generation and amalgamate with the main LEV. At $\mathrm{Re}_c = 21\,000$, the flow field is dominated by small-scale turbulence.

To determine the optimal Reynolds-number for the use of the LEV, we have performed additional simulations to the angle of attack of $\alpha = 25^\circ$ at Reynolds-numbers $\mathrm{Re}_c = 1000$, 4000, and 10 000 and determined the maximum transient lift coefficient that has been attained. Figure 6 shows these

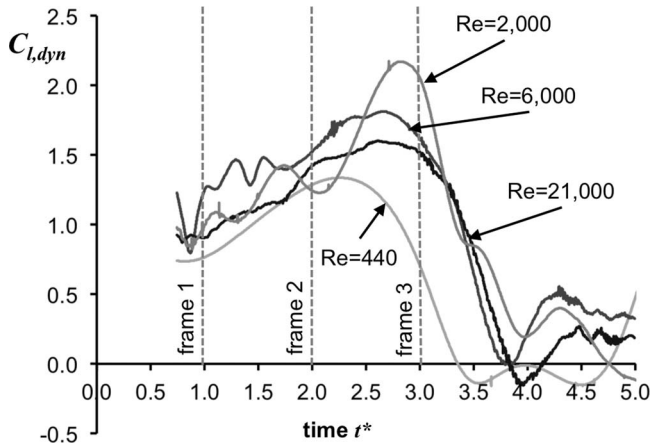

FIG. 4. Lift generated by the dynamic leading edge vortex $C_{l,\,dyn}(t) = C_l(t) - C_{l,\,mean}$ after the completion of the pitch-up motion. Frames 1 to 3 denote the instances to the corresponding images from Figure 3.

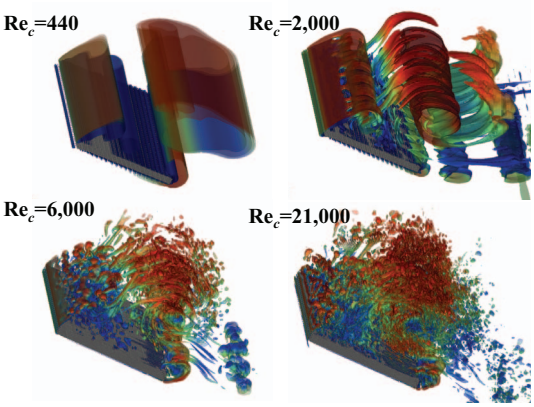

FIG. 5. Flow visualization of the three-dimensional vortex structure of the LEV using isosurfaces of the q-criterion[43] coloured with the velocity magnitude at $t^* = 3.0$.

results. The data suggest that at a Reynolds-number of $\mathrm{Re}_c = 2000$ optimal use of the LEV is made in terms of lift.

While the maximum lift is one important parameter, a better measure of aerodynamic efficiency is the lift-to-drag ratio C_l/C_d. In Figure 7 the lift in relation to drag is presented for four Reynolds-numbers and angles of attack ranging from $\alpha = 5^\circ$ to $\alpha = 30^\circ$. The time-averaged steady state values correspond to those of a flat plate in a freestream. The maximum lift-to-drag values are taken from the transient data during the passing of the LEV. It can be seen, that the lift-to-drag ratio due to the LEV is drastically higher than that of the steady state. It can also be noted that the curves for $\mathrm{Re}_c = 2000$–$21\,000$ are practically identical, especially at lift coefficients lower than 2.5. While the lower Reynolds-number of $\mathrm{Re}_c = 2000$ attains higher lift values, it achieves that only with a higher drag penalty. It is interesting to note that the highest absolute lift coefficients can be obtained at $Re_c = 6000$, albeit with a high drag penalty. At very low Reynolds-numbers, though, the viscosity plays a more important role and creates additional drag while not permitting the LEV to be fully developed. Hence, at low Reynolds-numbers the lift-to-drag ratio drops.

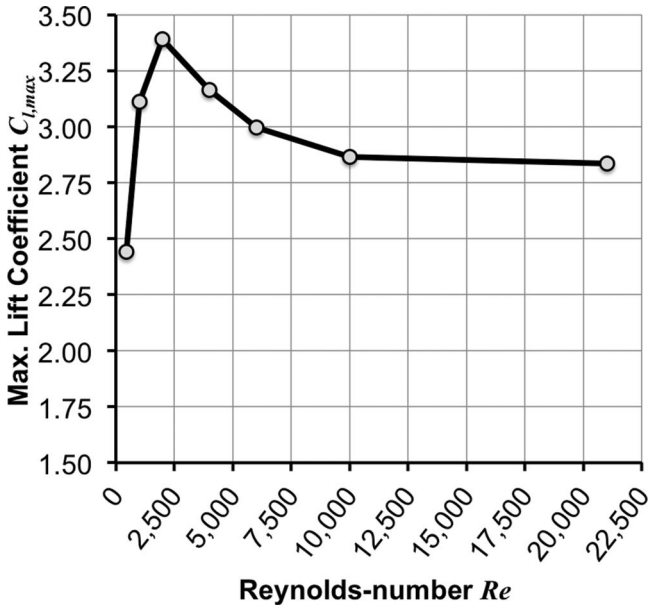

FIG. 6. Maximum transient lift-coefficient in dependence of Reynolds-number for an angle of attack of $\alpha = 25^\circ$.

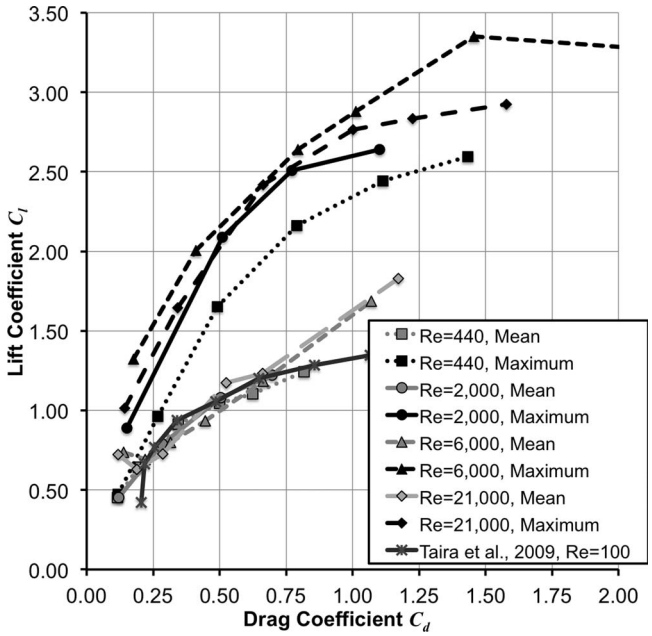

FIG. 7. Comparison of lift and drag values. Gray shaded lines: Time-averaged steady state values and literature data from Taira *et al.*;[44] Black lines: Transient maximum values during the creation of the LEV.

V. CONCLUSION

In this study, we have studied numerically the role of the Reynolds-number on the lift created by a leading edge vortex. Our results suggest that an optimal Reynolds-number exists that maximizes the lift generated by the LEV. The optimal Reynolds-number is determined by the fact that the viscosity needs to be sufficiently low to not disturb the generation of the LEV, but sufficiently large to inhibit the generation of small-scale turbulence that in turn disturb the coherence of the main LEV. While an optimal Reynolds-number can be found for the maximum lift generated by a LEV, the lift-to-drag ratio seems to be largely independent of the Reynolds-number at sufficiently high Reynolds-numbers. The lift-to-drag curves of the maximum lift-to-drag obtained by the LEV are nearly identical at Reynolds-numbers $Re_c \geq 2000$. At low Reynolds-numbers, the viscous effects result in reduced aerodynamic efficiency.

We have identified the influence of the Reynolds-number on the lift-enhancing effects of the LEV. The fact that the lift-to-drag ratio is independent of the Reynolds-number at higher Reynolds-number, may explain the fact that a wide variety of natural flyers use the LEV for flight. It also provides the opportunity of enhancing the aerodynamic efficiency for a variety of sizes of micro air vehicles.

[1] T. J. Mueller and J. D. DeLaurier, "An overview of micro air vehicle aerodynamics," in *Fixed and Flapping Wing Aerodynamics for Micro Air Vehicle Applications* (AIAA, Reston, VA, USA, 2001), Vol. 195, pp. 1–10.
[2] J. Schlüter, "Lift enhancement at low Reynolds-numbers using self-activated movable flaps," J. Aircr. **47**(1), 348–351 (2010).
[3] M. S. Selig, J. J. Guglielmo, A. P. Broern, and P. Giguere, "Experiments on airfoils at low Reynolds numbers," AIAA Paper No. 1996-0062, 1996.
[4] A. Azuma, *The Biokinetics of Flying and Swimming*, 2nd ed., AIAA Educators Series (AIAA, Reston 2006).
[5] W. Shyy, *Aerodynamics of Low Reynolds Number Flyers* (Cambridge University Press, New York, 2008).
[6] M. H. Dickinson, F. O. Lehmann, and S. P. Sane, "Wing rotation and the aerodynamic basis of insect flight," Science **284**, 1954–1960 (1999).
[7] T. Weis-Fogh, "Quick estimates of flight fitness in hovering animals, including novel mechanisms for lift production," J. Exp. Biol. **59**, 169–230 (1973), http://jeb.biologists.org/content/59/1/169.short.
[8] T. Maxworthy, "Experiments on the Weis-Fogh mechanism of lift generation by insects in hovering flight. Part 1. Dynamics of the 'fling'," J. Fluid Mech. **93**, 47–63 (1979).
[9] R. B. Srygley and A. L. R. Thomas, "Unconventional lift-generating mechanisms in free-flying butterflies," Nature (London) **420**, 660–664 (2002).
[10] D. R. Warrick, B. W. Tobalske, and D. R. Powers, "Aerodynamics of the hovering hummingbird," Nature (London) **435**, 1094–1097 (2005).

[11] F. T. Muijres, L. C. Johansson, R. Barfield, M. Wolf, G. R. Spedding, and A. Hedenström, "Leading-edge vortex improves lift in slow-flying bats," Science **319**, 1250–1253 (2008).
[12] D. Lentink, W. B. Dickson, J. L. van Leeuwen, and M. H. Dickinson, "Leading-edge vortices elevate lift of autorotating plant seeds," Science **324**, 1438–1440 (2009).
[13] C. P. Ellington, C. Van den Berg, A. P. Willmott, and A. L. R. Thomas, "Leading-edge vortices in insect flight," Nature (London) **384**, 626–630 (1996).
[14] M. Sun and J. Tang, "Unsteady aerodynamic force generation by a model fruit fly wing in flapping motion," J. Exp. Biol. **205**, 55–70 (2002), http://jeb.biologists.org/content/205/1/55.
[15] M. Kramer, "Zeitschrift für Flugtechnik und Motorluftschiffahrt," Zeitschrift für Flugtechnik und Motorluftschiffahrt **23**(7), 185–189 (1932).
[16] C. Han, J. Ahn, J. Cho, and Y. Moon, "Unsteady aerodynamic analysis of oscillating flat plate," AIAA Paper No. 2003-3674, 2003.
[17] C. Kang, H. Aono, P. Trizila, Y. Baik, J. M. Rausch, L. Bernal, M. V. Ol, and W. Shyy, "Modeling of pitching and plunging airfoils at Reynolds number between 1×10^4 and 6×10^4," AIAA Paper No. 2009-4100, 2009.
[18] Y. S. Baik, J. M. Rausch, and L. Bernal, "Experimental investigation of pitching and plunging airfoils at Reynolds number between 1×10^4 and 6×10^4," AIAA Paper No. 2009-4030, 2009.
[19] J. D. Eldredge and C. Wang, "High-fidelity simulations and low-order modeling of a rapidly pitching plate," AIAA Paper No. 2010-4281, 2010.
[20] M. V. Ol, A. Altman, J. D. Eldredge, D. J. Garmann, and Y. Lian, "Resume of the AIAA FDTC low Reynolds number discussion group's canonical cases," AIAA Paper No. 2010-1085, 2010.
[21] M. R. Visbal and J. S. Shang, "Investigation of the flow structure around a rapidly pitching airfoil," AIAA J. **27**(8), 1044–1051 (1988).
[22] M. M. Koochesfahani and V. Smiljanovski, "Initial acceleration effects on flow evolution around airfoils pitching to high angles of attack," AIAA J. **31**(8), 1529–1531 (1993).
[23] D. Lentik and M. H. Dickinson, "Rotational accelerations stabilize leading edge vortices on revolving fly wings," J. Exp. Biol. **212**, 2705–2719 (2009).
[24] W. Shyy and H. Liu, "Flapping wings and aerodynamic lift: The role of leading-edge vortices," AIAA J. **45**(12), 2817–2819 (2007).
[25] M. Germano, U. Piomelli, P. Moin, and W. Cabot, "A dynamic subgrid-scale eddy viscosity model," Phys. Fluids A **3**(7), 1760–1765 (1991).
[26] D. K. Lilly, "A proposed modification of the Germano subgrid-scale closure method," Phys. Fluids **4**, 633–635 (1992).
[27] C. S. Peskin, "Flow patterns around heart valves: a digital computer method for solving the equations of motion," Ph.D. dissertation, Yeshiva University, 1972.
[28] H. S. Udaykumar, R. Mittal, P. Rampunggoon, and A. Khanna, "A sharp interface cartesian grid method for simulating flows with complex moving boundaries," J. Comput. Phys. **174**, 345–380 (2001).
[29] E. A. Fadlun, R. Verzicco, R. Orlandi, and J. Mohd-Yusof, "Combined immersed-boundary finite-difference methods for three-dimensional complex flow simulations," J. Comput. Phys. **161**, 35–60 (2000).
[30] R. Verzicco, M. Fatica, G. Iaccarino, P. Moin, and B. Khalighi, "Large eddy simulation of a road vehicle with drag-reduction devices," AIAA J. **40**(12), 2447–2455 (2002).
[31] R. Verzicco, M. Fatica, G. Iaccarino, and P. Orlandi, "Flow in an impeller-stirred tank using an immersed-boundary method," AIChE J. **50**(6), 1109–1118 (2004).
[32] J. Mohd-Yusof, "Combined immersed boundary/B-spline methods for simulation of flow in complex geometries," *Annual Research Briefs*, Center for Turbulence Research, Stanford University, 1997, pp. 317–328.
[33] X. Q. Zhang, P. Theissen, and J. U. Schlüter, "A Lagrangian method for the treatment of freshly cleared cells in immersed boundary techniques," Int. J. Comput. Fluid Dyn. **23**(9), 667–670 (2009).
[34] C. Pierce and P. Moin, "Large eddy simulation of a confined coaxial jet with swirl and heat release," AIAA Paper No. 98-2892, 1998.
[35] C. D. Pierce, "Progress-variable approach for large-eddy simulation of turbulent combustion," Ph.D. dissertation, Stanford University, Stanford, CA, 2001.
[36] C. D. Pierce and P. Moin, "Method for generating equilibrium swirling inflow conditions," AIAA J. **36**(7), 1325–1327 (1998).
[37] J. U. Schlüter, "Static control of combustion oscillations by coaxial flows: An LES investigation," J. Propul. Power **20**(3), 460–467 (2004).
[38] J. U. Schlüter, H. Pitsch, and P. Moin, "Large eddy simulation inflow conditions for coupling with Reynolds-averaged flow solvers," AIAA J. **42**(3), 478–484 (2004).
[39] J. U. Schlüter, H. Pitsch, and P. Moin, "Outflow conditions for integrated large-eddy simulation/Reynolds-averaged Navier-Stokes simulations," AIAA J. **43**(1), 156–164 (2005).
[40] X. Q. Zhang, P. Theissen, and J. U. Schlüter, "Towards simulation of flapping wings using immersed boundary method," Int. J. Numer. Methods Fluids (in press).
[41] X. Q. Zhang, V. Chai, and J. U. Schlüter, "Reynolds-number dependency of the leading edge vortex on a fast pitch-up flat plate," AIAA Paper No. 2011-3794, 2011.
[42] H. A. Wagner, "Über die Entstehung des dynamischen Auftriebes von Tragflügeln," Z. Angew. Math. Mech. **5**, 17–35 (1925).
[43] G. Haller, "An objective definition of a vortex," J. Fluid Mech. **525**, 1–26 (2005).
[44] K. Taira, B. Dickson, T. Colonius, and M. H. Dickinson, "Unsteadiness in flow over a flat plate at angle-of-attack at low Reynolds numbers," AIAA Paper No. 2007-0710, 2007.